PROCEEDINGS OF THE ROYAL SOCIETY B

Proc. R. Soc. B (2012) **279**, 237–246
doi:10.1098/rspb.2011.0599
Published online 15 June 2011

A stem-deuterostome origin of the vertebrate pharyngeal transcriptional network

J. Andrew Gillis*,†, Jens H. Fritzenwanker‡ and Christopher J. Lowe*,‡

Department of Organismal Biology and Anatomy, University of Chicago, 1027 East 57th Street, Chicago, IL 60637, USA

Hemichordate worms possess ciliated gills on their trunk, and the homology of these structures with the pharyngeal gill slits of chordates has long been a topic of debate in the fields of evolutionary biology and comparative anatomy. Here, we show conservation of transcription factor expression between the developing pharyngeal gill pores of the hemichordate *Saccoglossus kowalevskii* and the pharyngeal gill slit precursors (i.e. pharyngeal endodermal outpockets) of vertebrates. Transcription factors that are expressed in the pharyngeal endoderm, ectoderm and mesenchyme of vertebrates are expressed exclusively in the pharyngeal endoderm of *S. kowalevskii*. The pharyngeal arches and tongue bars of *S. kowalevskii* lack *Tbx1*-expressing mesoderm, and are supported solely by an acellular collagenous endoskeleton and by compartments of the trunk coelom. Our findings suggest that hemichordate and vertebrate gills are homologous as simple endodermal outpockets from the foregut, and that much vertebrate pharyngeal complexity arose coincident with the incorporation of cranial paraxial mesoderm and neural crest-derived mesenchyme within pharyngeal arches along the chordate and vertebrate stems, respectively.

Keywords: hemichordate; pharyngeal gill slit; pharyngeal arch; endodermal outpocket; evolution; deuterostome

1. INTRODUCTION

Pharyngeal gill slits are one of the four classic chordate anatomical synapomorphies (along with a dorsal hollow nerve cord, a notochord and a post-anal tail [1]), and feature prominently in most narratives or scenarios of vertebrate evolution and diversification [2–6] (discussed in [7]). However, gill slits (or gill pores) are also present in hemichordate worms [8], and gill-slit-like structures have been described in putative stem-echinoderms [9] and stem-deuterostomes [10]. This suggests that, far from being a chordate synapomorphy, pharyngeal gill slits are a primitive feature of deuterostomes that has been lost in echinoderms and *Xenoturbella* (and possibly also in acoelomorph flatworms [11]). It follows from this that, as the only extant non-chordate deuterostome taxon to possess gill slits, hemichordates represent a crucial phylogenetic data point for studies on the evolutionary origin of the vertebrate pharynx and its derivatives [12].

The earliest morphological indication of gill slit formation in vertebrates is the appearance of pharyngeal endodermal outpockets (reviewed in [13]). These outpockets evaginate from the foregut, contact the body wall ectoderm and fuse, giving rise to a slit (gill slit) in the wall of the pharynx. One consequence of the iterative perforation of pharyngeal gill slits is the formation of mesenchyme-filled epithelial columns (pharyngeal arches) between the slits. These arches are lined laterally by ectoderm, medially by endoderm and contain a discrete central core of cranial paraxial mesoderm surrounded by cranial neural crest-derived mesenchyme [14,15]. In all vertebrates, pharyngeal arch ectoderm gives rise to the sensory neurons of the epibranchial ganglia [16,17], while pharyngeal arch mesoderm and neural crest-derived mesenchyme give rise to the musculature and skeletal elements of the pharynx, respectively [18,19]. Finally, pharyngeal arch endoderm gives rise to the endocrine glands of the pharynx—the thymus, thyroid and (in amniotes) parathyroid glands [20,21].

Early gill slit morphogenesis in hemichordates closely resembles that of vertebrates. Hemichordates possess a tripartite bodyplan (figure 1*a*), with an anterior muscular proboscis (prosome), a middle collar (mesosome) and a posterior trunk (metasome), and gill slits form exclusively on the metasome. Endodermal outpockets evaginate from the gut, contact metasome surface ectoderm and fuse to form pharyngeal pores, which are separated by pharyngeal arches [8]. However, hemichordates do not exhibit the complex sequence of pharyngeal arch organogenesis that is seen in vertebrates. In some pterobranch hemichordates, gills remain as simple ciliated pores that open directly into the foregut, and lack any form of endoskeletal support [22]. In enteropneust hemichordates, the gills open externally as simple pores (figure 1*b*), but are subdivided internally by an epithelial 'tongue bar'

* Authors for correspondence (jag93@cam.ac.uk; clowe@stanford.edu).
† Present address: Department of Physiology, Development and Neuroscience, University of Cambridge, Anatomy Building, Downing Street, Cambridge CB2 3DY, UK.
‡ Present address: Hopkins Marine Station, Stanford University, 120 Oceanview Boulevard, Pacific Grove, CA 93950, USA.

Electronic supplementary material is available at http://dx.doi.org/10.1098/rspb.2011.0599 or via http://rspb.royalsocietypublishing.org.

Received 20 March 2011
Accepted 23 May 2011

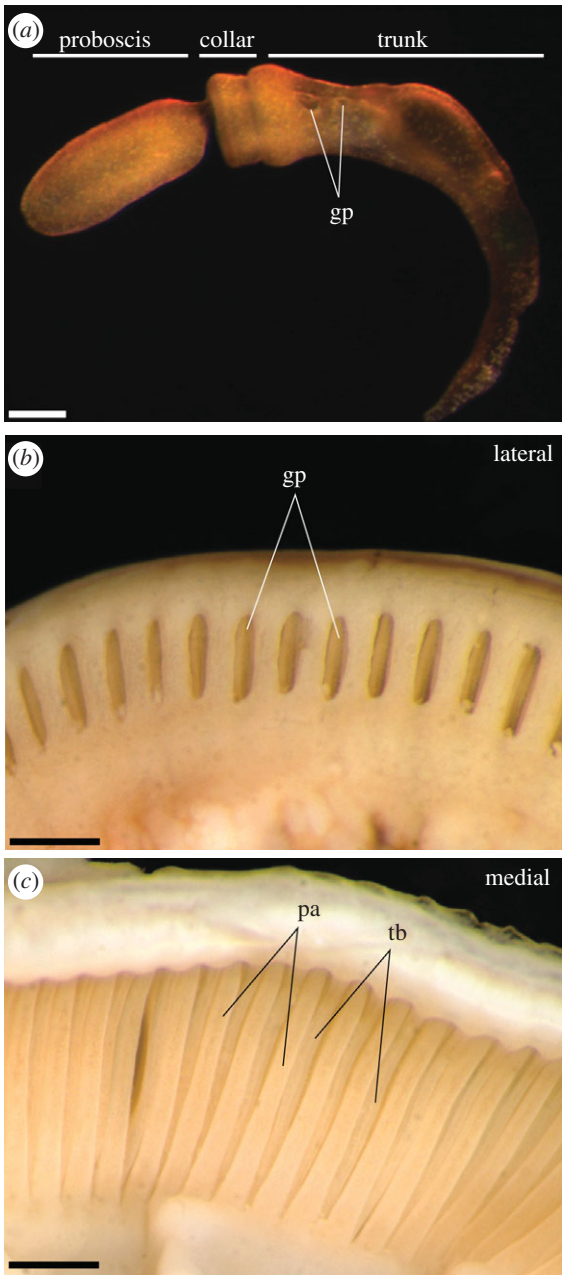

Figure 1. Anatomical overview of the juvenile and adult *Saccoglossus kowalevskii* pharyngeal gills. (*a*) *S. kowalevskii* exhibits a tripartite body organization, with an anterior proboscis, a middle collar and a posterior trunk. In juveniles, gills form as simple pores on the trunk. (*b*) A lateral view of the adult *S. kowalevskii* trunk shows the gills opening externally as simple pores. (*c*) A medial view of the adult *S. kowalevskii* trunk shows the alternating arrangement of internal pharyngeal arches and tongue bars that bound and divide, respectively, each pharyngeal gill slit. Scale bars: (*a*) 250 µm; (*b*,*c*) 1 mm. gp, gill pore; pa, pharyngeal arch; tb, tongue bar.

that descends by evagination from the dorsal wall of the slit. This yields an arrangement of alternating pharyngeal arches and tongue bars, interspersed with narrow, ciliated slits that open into the pharyngeal cavity and function as a feeding apparatus (figure 1*c*) [23]. The enteropneust pharyngeal apparatus is supported by an endodermally secreted, acellular collagenous endoskeleton, which takes the form of a series of inverted trident structures, with arms descending into each pharyngeal arch and tongue bar [24–28] (see also figure 2*e*,*f*).

A number of transcription factors—including *Pax1*, *Pax9*, *Eya1*, *Six1*, *Hox1*, *Hox3*, *FoxC* and *Tbx1*—are expressed during early pharyngeal arch development in mammals (see below). A complex network of regulatory links between these factors is now emerging, and null mutations of most of these genes results in loss or abnormal development of the pharyngeal arches and/or their derivatives—including aplasia or hypoplasia of the thyroid, thymus and parathyroid [29–31]. Did these molecular interactions arise in conjunction with the origin of anatomical complexity in the vertebrate pharynx, or did novel vertebrate pharyngeal arch derivatives arise within the context of an ancient, pre-existing pharyngeal gene-regulatory network?

We sought to test the extent to which the vertebrate pharyngeal transcriptional network was assembled in the last common ancestor of deuterostomes, by characterizing the expression of hemichordate orthologues of these transcription factors during gill pore development in the enteropneust worm, *Saccoglossus kowalevskii*. Interestingly, we find conserved expression of five of these factors in the endoderm of the morphologically simple pharyngeal gill pores of *S. kowalevskii*. Our findings suggest that a sophisticated transcriptional network functioned primitively to regulate endodermal outpocketing in the pharynx of the last common ancestor of deuterostomes. We suggest that much vertebrate pharyngeal complexity arose through novel tissue interactions—interactions that were enabled by the stepwise incorporation into the pharyngeal arches of paraxial mesoderm and neural crest-derived mesenchyme, along the chordate and vertebrate stems, respectively.

2. MATERIAL AND METHODS

(a) *Animal collection, husbandry and fixation*

Saccoglossus kowalevskii adults were collected in September 2008 from Waquoit Bay, near Woods Hole, MA, USA. Embryos were acquired, maintained and fixed as previously described [32]. Juvenile cultures were maintained in glass dishes of filtered sea water with a reptile sand substrate at ambient temperature (approx. 21°C), and were fed DT's Premium Reef Blend phytoplankton following daily water changes. Amphioxus (*Branchiostoma lanceolatum*) adults were provided by Hector Escriva, and were fixed as previously described [32]. *Scyliorhinus canicula* embryos were obtained from the CNRS Station Biologique in Roscoff, France, and were fixed as previously described [33].

(b) *Probes*

Antisense riboprobes for *Pax1/9* (GenBank DQ869011), *Six1* (GenBank JN008939), *Eya* (GenBank JN008940), *FoxC* (GenBank EU932651), *Hox1* (GenBank AY313156), *Hox3* (GenBank NM_001164907) and *Tbx1* (GenBank GU076134) were transcribed using T7 RNA polymerase (Invitrogen) and digoxygenin- or fluorescein-labelled rNTPs (Roche), according to the manufacturer's instructions.

(c) *mRNA* in situ *hybridization*

In situ hybridizations for neurula-stage embryos were performed as described by Zou *et al.* [31]. *In situ* hybridizations for one to four gill-slit-stage juveniles were performed similarly, but with the following modification: following rehydration from 100 per cent ethanol (EtOH), juveniles were treated with a 1 : 10 000 dilution of proteinase-K (Roche) for

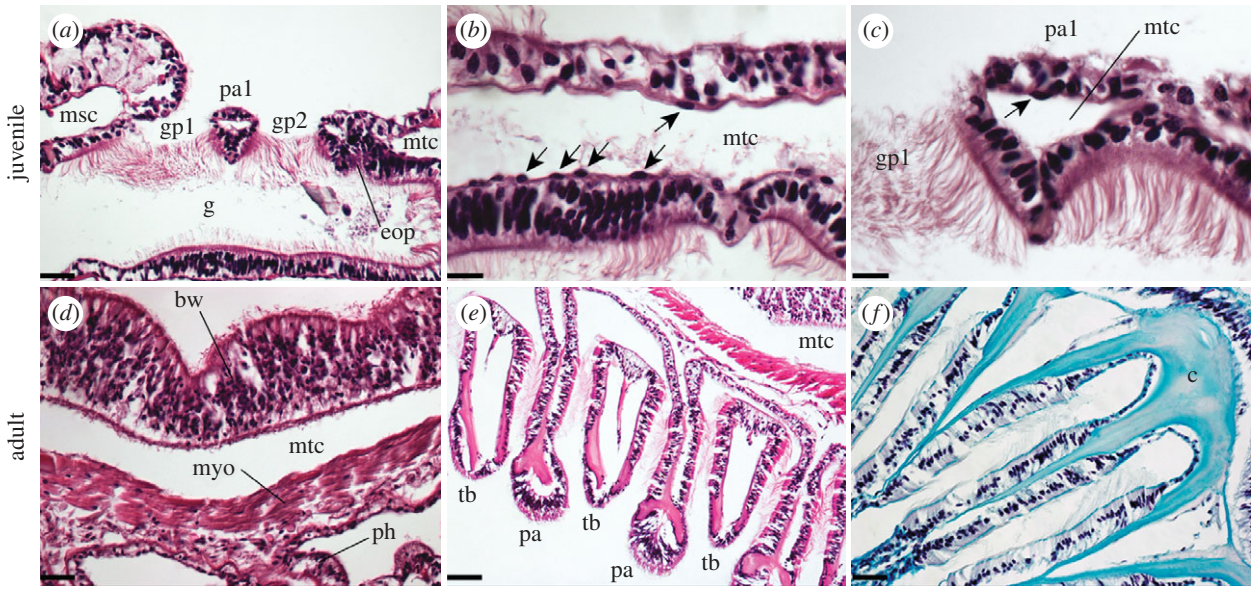

Figure 2. Pharyngeal histology in *Saccoglossus kowalevskii* (*a–c*) juveniles and (*d–f*) adults. (*a*) A horizontal section through a juvenile *S. kowalevskii* shows two perforated gill pores, with the third gill pore in the process of forming. Gill pore formation occurs by fusion of an endodermal outpocket with the body wall ectoderm, and this results in the trapping of a compartment of the metacoel within the pharyngeal arch between two gill pores. (*b*) The metacoel is sparsely lined by a thin mesothelium that sits subjacent to the body wall and gut basal lamina, and (*c*) these coelom-lining cells are occasionally trapped within the coelomic compartment of a pharyngeal arch. (*d*) In *S. kowalevskii* adults, the cells lining the metacoel give rise to a myoepithelium. (*e*) A ventral cross-section through the pharyngeal arches of *S. kowalevskii* reveals the arrangement of alternating pharyngeal arches and tongue bars. (*f*) The *Saccoglossus* pharyngeal endoskeleton is acellular, and is secreted by the endoderm within each pharyngeal arch and tongue bar. Scale bars: (*a*) 30 μm; (*b*,*c*) 15 μm; (*d*) 20 μm; (*e*) 25 μm; (*f*) 10 μm. bw, body wall; c, collagenous endoskeleton; eop, endodermal outpocket; gp1–2, gill pores 1–2; g, gut; msc, mesocoel; mtc, metacoel; myo, myoepithelium; pa, pharyngeal arch; pa1, pharyngeal arch 1; ph, pharyngeal endoderm; tb, tongue bar. Anterior is to the left in all images, except for (*f*), where anterior is down.

17 min at room temperature. Juveniles were then post-fixed in formaldehyde, and hybridization was carried out as previously described [31].

(d) *Immunohistochemistry*

Juveniles were rehydrated from 100 per cent EtOH in 1X PBS + 0.1% Triton X-100 (PBSTr), and rinsed 3 × 10 min in PBSTr. Blocking was carried out in 5 per cent goat serum in PBSTr for more than 1 h at room temperature, and primary antibody incubation was carried out at 4°C overnight. Monoclonal anti-acetylated tubulin produced in mouse was diluted 1 : 200 in 5 per cent goat serum/PBSTr. Following primary antibody incubation, animals were rinsed 3 × 30 min in PBSTr at room temperature. Secondary antibody incubation (Alexafluor 546 rabbit-anti-mouse IgG, diluted 1 : 50 in 5% goat serum in PBSTr) was carried out for 4 h at room temperature. Animals were then rinsed 3 × 30 min in PBSTr at room temperature, and stored in PBSTr at 4°C prior to photography. Embryos were mounted in Prolong Gold antifade mounting medium (Molecular Probes) for imaging.

(e) *Histology*

From 100 per cent EtOH, *S. kowalevskii* juveniles and adults, *B. lanceolatum* adults and *Scyliorhinus canicula* embryos were embedded in paraffin (Fisher) following infiltration with Citrisolve (Fisher). In a 58°C paraffin oven, specimens were infiltrated for 3 × 24 h in Citrisolve, 2 × 24 h in 1 : 1 Citrisolve : paraffin and 3 × 24 h in paraffin. Specimens were then embedded in fresh paraffin and left to harden for 24 h prior to sectioning. Sections of 5 μM were cut on a Microm HM330 rotary microtome, and these sections were mounted on glass slides and stained with either a standard or a modified haematoxylin and eosin staining protocol [33]. Slides were cover-slipped with Permount (Fisher) prior to imaging.

3. RESULTS

(a) *Gill pore perforation and pharyngeal arch histology in* Saccoglossus kowalevskii

The gill pores of *S. kowalevskii* are heavily ciliated, and stain positively for acetylated tubulin. Acetylated tubulin immunoreactivity may therefore be used to observe the timing of gill pore perforation and morphogenesis (see electronic supplemental material). *Saccoglossus kowalevskii* embryos hatch from their vitelline envelopes at 5–5.5 days post-fertilization (dpf). At this stage, the first gill pore has already perforated anterior to the ciliary band (see electronic supplementary material, figure S1*a*). At approximately 7–9 dpf, the second gill pore perforates (see electronic supplementary material, figure S1*b*). At this stage, the first gill pore has enlarged and begins to adopt a U-shaped morphology as a result of downward evagination of the dorsal gill pore epithelium. This is the earliest indication of tongue bar development in the first gill pore. At approximately 10–11 dpf, the third gill pore perforates (see electronic supplementary material, figure S1*c*). The fourth gill pore perforates at approximately 20–23 dpf (see electronic supplementary material, figure S1*d*). By this time, the first two gill pores show early signs of tongue bar evagination, while the third and fourth gill pores remain as simple, circular pores. At this gross morphological level of analysis, gill pore perforation in *S. kowalevskii* appears to be bilaterally

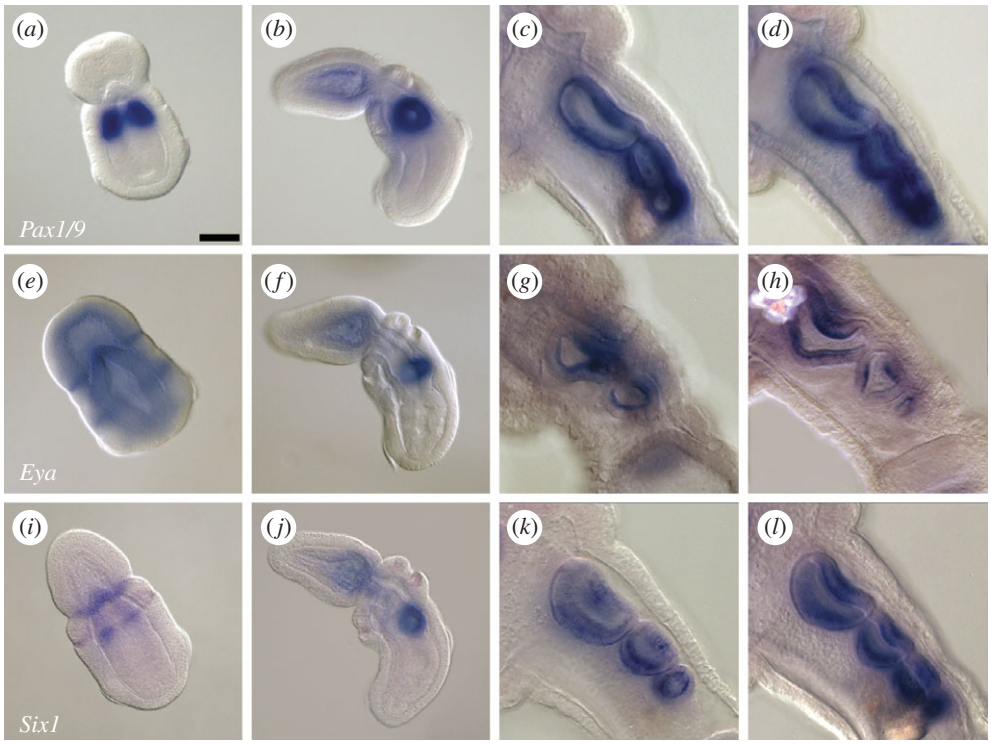

Figure 3. (*a–d*) *Pax1/9*, (*e–h*) *Eya* and (*i–l*) *Six1* are expressed in the developing pharyngeal gill pores of *Saccoglossus kowalevskii*. *Pax1/9* is expressed in the presumptive first gill pore endoderm at (*a*) the neurula stage, and in the epithelium of the gill pores at the (*b*) one-, two- (not shown), (*c*) three- and (*d*) four-gill-pore stages. *Eya* is expressed in the presumptive first gill pore endoderm at (*e*) the neurula stage, and in the innermost epithelium of the gill pores at the (*f*) one-, (*g*) two-, (*h*) three- and four- (not shown) gill-pore stages. *Six1* is expressed in the proboscis–collar boundary and presumptive first gill pore endoderm at (*i*) the neurula stage, and in the epithelium of the gill pores at the (*j*) one-, two- (not shown), (*k*) three- and (*l*) four-gill-pore stages. In all images, animals are oriented with anterior to the upper left. Scale bar in (*a*): 50 μm; all images to same scale.

symmetric, with no evidence of pronounced left–right asymmetry (i.e. as is seen in amphioxus [34]).

In the trunk of *S. kowalevskii* juveniles, the space between the ciliated gut endoderm and the body wall ectoderm is occupied by a mesodermally derived trunk coelom (the metacoel). As *S. kowalevskii* gill pores form by the fusion of ciliated endodermal outpockets with trunk ectoderm, each gill pore must perforate the metacoel, and each pharyngeal arch therefore encloses a small metacoel-derived coelomic space (figure 2*a*). The juvenile metacoel is lined by a thin mesothelium—presumably of mesodermal origin—which lies subjacent to the body wall and gut basal lamina (figure 2*b*). The pharyngeal arches of *S. kowalevskii* juveniles are epithelial structures, and are effectively devoid of mesoderm, with the exception of small numbers of coelom-lining mesothelial cells that may become trapped within the pharyngeal arch during gill slit formation (figure 2*c*). In *S. kowalevskii* adults, cells lining the metacoel give rise to the muscular lining of the coelom (figure 2*d*)—the myoepithelium [22]. The endoderm of the pharynx secretes an acellular collagenous endoskeleton, which takes the form of an inverted trident. The central branch of the trident descends into a pharyngeal arch, while the lateral branches descend into the two adjacent tongue bars (figure 2*e*,*f*).

(b) Pax1/9, Eya *and* Six1 *expression*

In E9.5–10.5 mouse embryos, the homeobox transcription factors *Pax1* and *Pax9* are co-expressed in the pharyngeal endodermal outpockets [35,36], while *Eya1* and *Six1* are co-expressed in pharyngeal endoderm, ectoderm and mesenchyme [29]. Mutant analysis has revealed that these genes form a *Pax–Eya–Six* regulatory hierarchy, which is required for the normal development of the parathyroid and thymus [29,31]. We therefore examined the expression patterns of *Pax1/9*, *Eya* and *Six1* orthologues during gill pore development in *S. kowalevskii*.

Expression of *Pax1/9* has previously been reported in the first gill pore of *S. kowalevskii* [37], as well as in the adult gill epithelium of *S. kowalevskii* [28] and *Ptychodera flava* [38]. We note that *Pax1/9* is strongly expressed in the presumptive first gill pore endoderm of neurula stage embryos, prior to endodermal outpocketing (figure 3*a*) [37]. This expression is maintained in the ring of epithelium surrounding the first gill pore following perforation (figure 3*b*) [37]. *Pax1/9* is also expressed in the epithelium of the second, third and fourth (figure 3*c*,*d*) gill pores. *Pax1/9* expression is maintained throughout the gill epithelium following perforation of each gill pore.

At the neurula stage, *Eya* is expressed in an ectodermal band at the proboscis–collar boundary, and in the ectoderm and endoderm at the level of the presumptive first gill pore (figure 3*e*). Like *Pax1/9* and *Six1* (see below), *Eya* expression is detected exclusively in the gill pore epithelium at the one-, two- and three-gill-pore stages (figure 3*f*,*h*). Unlike *Pax1/9* and *Six1*, however, *Eya* expression appears to be restricted to the innermost layer of the gill slit epithelium.

Six1 is expressed at late neurula stage in the presumptive first gill pore endoderm and in an ectodermal ring at the

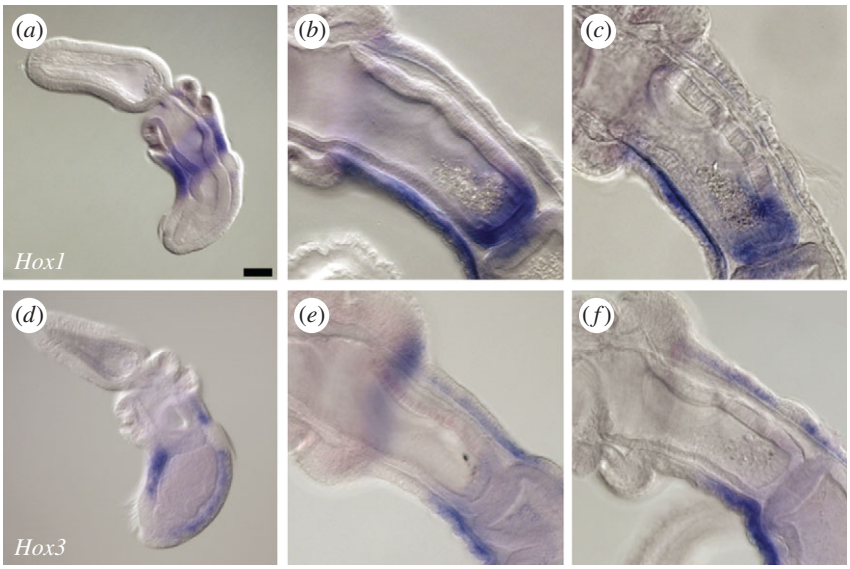

Figure 4. (*a–c*) *Hox1*, but not (*d–f*) *Hox3*, is expressed in the developing pharynx of *Saccoglossus kowalevskii*. At the (*a*) one-gill-pore stage, *Hox1* is expressed in the ectoderm and endoderm at the level of the first pore. This expression is subsequently extinguished, and by the (*b*) three- and (*c*) four-gill-pore stages *Hox1* is expressed in the posterior pharyngeal endoderm and in the ventral nerve cord. At the (*d*) one-gill-pore stage, *Hox3* is expressed in the dorsal and ventral ectoderm, but not in the endoderm of the first gill pore. At the (*e*) three- and (*f*) four-gill-pore stages, *Hox3* expression is detected in the dorsal and ventral nerve cords, but is not detected in the pharyngeal endoderm. In all images, animals are oriented with anterior to the upper left. Scale bar in (*a*): 50 μm; all images to same scale.

proboscis–collar boundary (figure 3*i*). *Six1* expression persists in the pharyngeal epithelium of the first gill pore after perforation (figure 3*j*). As with *Pax1/9*, *Six1* expression is detected in the pharyngeal epithelium surrounding the second, third and fourth gill pores (figure 3*k*,*l*). Expression persists in all gill pores at the four-gill-pore stage, with a slight downregulation of expression in the dorsal epithelium of the first and second gill pores on either side of the forming tongue bar (figure 3*l*).

(c) Hox1 *and* Hox3 *expression*

In mice, the homeobox transcription factors *Hoxa1*, *Hoxb1* and *Hoxa3* are expressed in the endoderm and neural-crest-derived mesenchyme of the third and fourth pharyngeal arches [39,40], and in $Hoxa1^{-/-}$/$Hoxb1^{-/-}$ and $Hoxa3^{-/-}$ mice, the parathyroid and thymus—which derive from the endoderm of the third and fourth pharyngeal pouches—fail to form [39,41]. In *S. kowalevskii*, we note the expression of *Hox1* in the ectoderm of the anterior metasome, approximately at the level of the presumptive first gill pore (data not shown; as previously reported [37,42]). At the one-gill-slit stage (figure 4*a*), *Hox1* expression is detected in the ectoderm skirting the first gill pore, as well as in the endoderm immediately posterior to the pore opening (marking the posterior boundary of the pharyngeal endoderm [42]). At the three-gill-slit stage, *Hox1* expression is restricted to the endoderm at the posterior boundary of the foregut, and to the ventral nerve cord (figure 4*b*). Ventral nerve cord expression of *Hox1* extends anteriorly to the level of the collar. Endodermal expression of *Hox1* remains restricted to the posterior pharynx at the four-gill-pore stage (figure 4*c*).

Unlike in vertebrates, *Hox3* expression is not detected in the pharyngeal endoderm of *Saccoglossus*. At neurula stage, *Hox3* is expressed in an ectodermal ring that sits posterior to the ectodermal ring of *Hox1* expression on the metasome (data not shown; as previously reported [42]). At the one-gill-pore stage, expression becomes focused along the dorsal and ventral midline (figure 4*d*). Ventral midline expression extends posteriorly to the ciliary band and anteriorly to the collar, while dorsal midline expression spans the entire length of the trunk. At the three-gill-pore stage (figure 4*e*) and four-gill-pore stage (figure 4*f*), *Hox3* expression remains restricted to the dorsal and ventral nerve cords, with dorsal cord expression extending anteriorly to the level of the collar, and ventral nerve cord expression extending anteriorly to the boundary between the first and second gill pores. No *Hox3* expression is detected in the pharyngeal endoderm.

(d) Tbx1 *and* FoxC *expression*

In mice, *Tbx1* is expressed in the endoderm and core mesoderm of the pharyngeal arches, and in the neural-crest-derived mesenchyme of the head [43]. $Tbx1^{-/-}$ mice phenocopy human DiGeorge syndrome and exhibit parathyroid and thymus hypoplasia [44]. Members of the *Forkhead box* (*Fox*) family of transcription factors act as upstream regulators of pharyngeal *Tbx1* expression. Pharyngeal endodermal expression of *Tbx1* is directly regulated by endodermal expression of *FoxA* [45], and compound $Foxc1^{-/-}$/$Foxc2^{-/-}$ mice exhibit a downregulation of pharyngeal mesoderm *Tbx1* expression and hypoplastic pharyngeal arches [46,47].

We found that *Tbx1* was not expressed in the pharyngeal region of *S. kowalevskii* at any stage. At neurula stage, *Tbx1* is expressed panectodermally, excluding the ciliary band (figure 5*a*). However, this panectodermal expression is extinguished by the stage at which the first gill pore has perforated (figure 5*b*), and no expression is detected in the pharyngeal region of juveniles at the two-, three- or four-gill-pore stages (figure 5*c*,*d*).

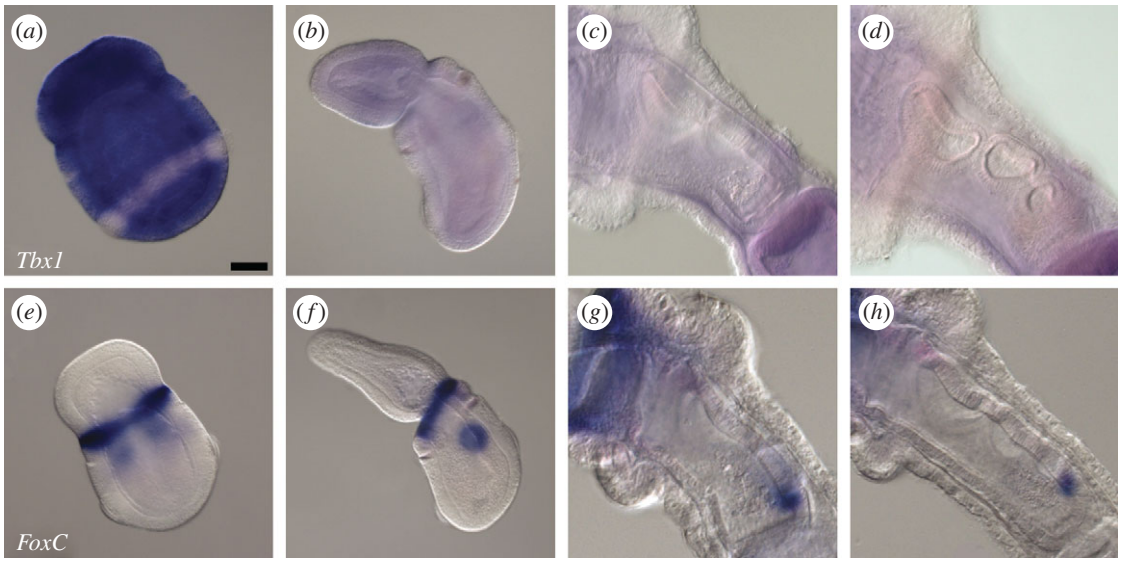

Figure 5. (*a–d*) *Tbx1* is not expressed in the pharyngeal gill pores or pharyngeal arches of *Saccoglossus kowalevskii*, though (*e–h*) *FoxC* is expressed in the gill pore epithelium. (*a*) At the neurula stage, *Tbx1* is expressed panectodermally, excluding the ciliary band. Expression of *Tbx1* is not detected at the (*b*) one-, two- (not shown), (*c*) three- or (*d*) four-gill-pore stages. (*e*) At the neural stage, *FoxC* is expressed at the presumptive proboscis–collar boundary, and in the presumptive first gill pore endoderm. Expression of *FoxC* is subsequently detected in the epithelium of the developing (*f*) first, second (not shown), (*g*) third and (*h*) fourth gill pores. In all images, animals are oriented with anterior to the upper left. Scale bar in (*a*): 50 μm. All images to same scale.

Expression of *FoxA* was also not detected in the pharyngeal endodermal outpockets of *S. kowalevskii* (data not shown). However, *FoxC* expression was detected during pharyngeal gill pore development in *S. kowalevskii*. At the neurula stage, we observed *FoxC* expression in an ectodermal ring at the proboscis–collar boundary, and also in the endoderm at the level of the presumptive first gill pore (figure 5*e*). This endodermal expression persists until perforation of the first gill pore (figure 5*f*), and a similar expression pattern is reiterated in the perforating second, third and fourth gill pores (figure 5*g*,*h*). However, unlike the expression of *Pax1/9*, *Six1* and *Eya* (which persist in the perforated gill pore epithelium), *FoxC* expression is extinguished from the gill pore epithelium shortly after perforation. Pharyngeal endodermal expression of *FoxC* has not been described previously in osteichthyans, but has been observed in the shark *Scyliorhinus canicula* [48].

4. DISCUSSION

The morphological disparity exhibited by chordate and hemichordate pharyngeal gills has raised questions about the level at which these structures may be considered homologous [22]. Here, we have shown that key elements of the vertebrate pharyngeal arch gene-regulatory network are conserved in the pharyngeal endodermal outpockets and gill pore epithelium of a hemichordate, *S. kowalevskii*. Specifically, we observe conserved co-expression of *Pax1/9*, *Eya* and *Six1* in the developing pharyngeal gill pores of *S. kowalevskii*. Given the co-expression and regulatory interaction of these factors in the pharyngeal endoderm of vertebrates [29,31] and the non-vertebrate chordate amphioxus [49,50], these findings suggest a deeply conserved role for a *Pax–Eya–Six* regulatory cascade in patterning the pharyngeal endoderm of deuterostomes. We also observe conserved posterior pharyngeal endodermal expression of *Hox1*. However, unlike in vertebrates, we find no evidence of pharyngeal *Hox3* expression, suggesting that the co-expression of *Hox1* and *Hox3* in pharyngeal endoderm might represent a chordate or vertebrate novelty. Finally, we do not observe pharyngeal expression of *Tbx1*, though we do observe gill slit expression of *FoxC*, which acts (probably indirectly) as an upstream regulator of *Tbx1* in vertebrate pharyngeal arch mesoderm. Taken together, these findings are indicative of a stem-deuterostome origin of some of the key molecular interactions that are involved in vertebrate pharyngeal patterning, and suggest that the roles of many of these transcription factors in vertebrate pharyngeal organogenesis (e.g. thyroid, thymus and parathyroid development) are secondary to a more primitive role in endodermal outpocketing and early gill slit morphogenesis.

In vertebrates, *Hox1* and *Hox3* paralogues play central but distinct roles in patterning the pharyngeal arches. *Hoxa1*, *Hoxb1* and *Hoxa3* are expressed in the third and fourth pharyngeal endodermal outpockets, and while *Hoxa1* and *Hoxb1* double-mutants exhibit defects in pharyngeal endodermal outpocketing [40,41], *Hoxa3* mutants undergo normal outpocketing, but subsequently exhibit a number of defects in posterior pharyngeal endodermal derivatives (including athymia, aparathyroidism and thyroid hypoplasia [39,51,52]). A conserved role for *Hox1* in patterning the posterior pharynx has been demonstrated in the cephalochordate amphioxus [50,53], and our demonstration that *Hox1* (but not *Hox3*) is expressed in the posterior pharyngeal endoderm in *Saccoglossus* suggests that this is probably a primitive feature of deuterostomes. The different phenotypes exhibited by *Hox1* and *Hox3* mutant mice (i.e. defective outpocketing versus defective organogenesis, respectively) may reflect a primitive function of *Hox1* as a regulator of endodermal outpocketing in deuterostomes, and a *Hox3* function in pharyngeal organogenesis that was acquired subsequently in vertebrates.

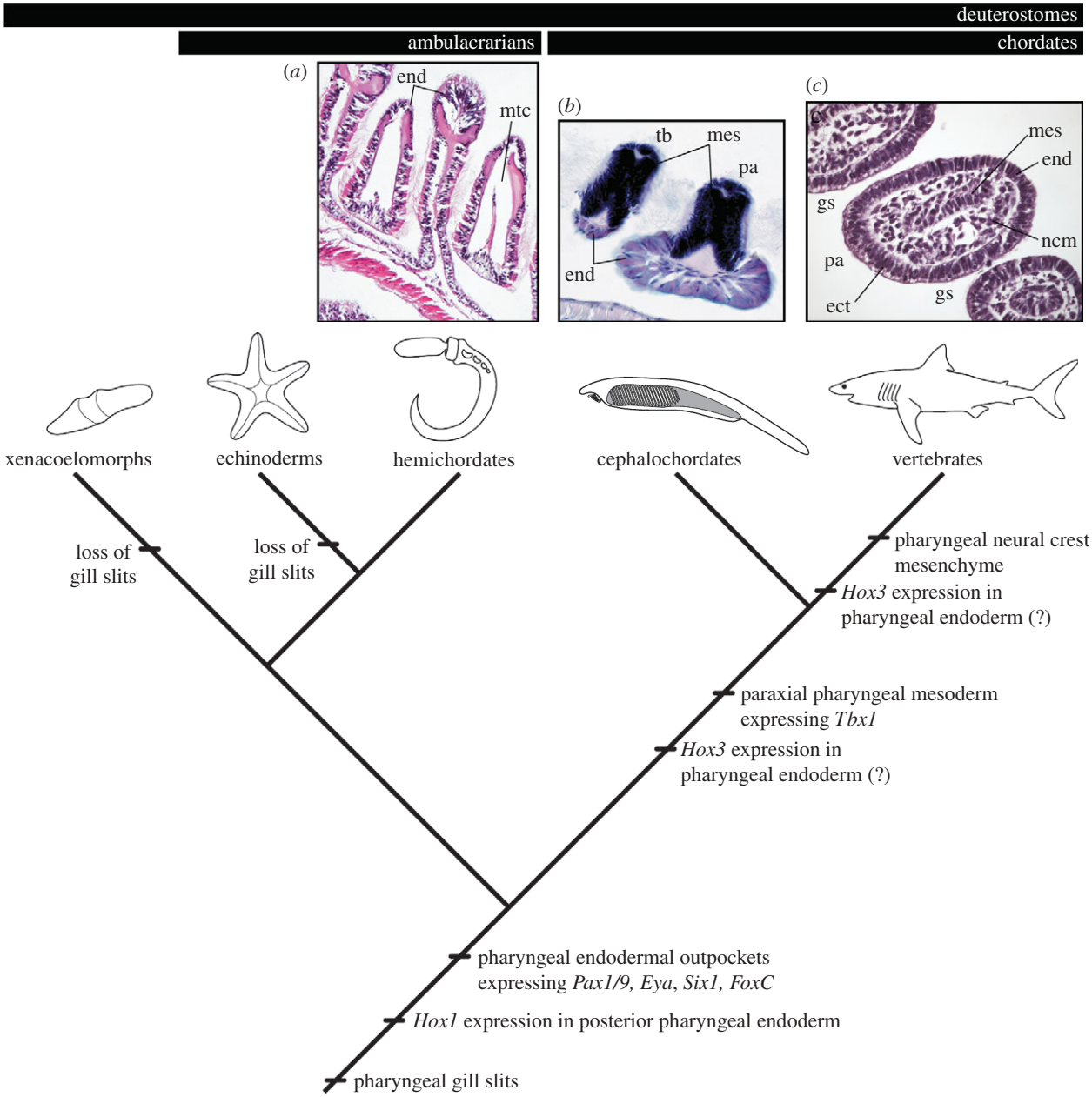

Figure 6. The evolution of deuterostome pharyngeal arches. Histological images are transverse sections through the pharyngeal arches of (*a*) *Saccoglossus kowalevskii*, (*b*) *Branchiostoma lanceolatum* and (*c*) *Scyliorhinus canicula*. Deuterostomes primitively possessed gill pores that formed from endodermal outpockets expressing *Pax1/9*, *Eya*, *Six1* and *FoxC*. Posterior pharyngeal endodermal expression of *Hox1*, alternating pharyngeal arches and tongue bars and an endodermally secreted, acellular collagenous pharyngeal skeleton, are also probably primitive deuterostome features. A *Tbx1*-expressing mesodermal contribution to the pharyngeal arches arose along the chordate stem, and a neural crest mesenchyme contribution to the pharyngeal arches arose along the vertebrate stem. *Hox3* expression in the pharyngeal endoderm arose along the chordate or vertebrate stem. ect, ectoderm; end, endoderm; gs, gill slit; mes, mesoderm; mtc, metacoel; ncm, neural-crest-derived mesenchyme; pa, pharyngeal arch; tb, tongue bar.

The T-box transcription factor *Tbx1* is expressed in the mesodermal core of the pharyngeal arches in all chordates examined to date, including mouse [43], lamprey [54] and amphioxus [55]. The absence of *Tbx1* expression in the pharyngeal arches of *S. kowalevskii* suggests that *Tbx1*-expressing pharyngeal mesoderm may have originated along the chordate stem. The forkhead transcription factors *FoxA*, *FoxC1* and *FoxC2* are known regulators of *Tbx1* expression in the mammalian head and pharyngeal arches. We did not detect *FoxA* expression in the pharyngeal gill pores of *S. kowalevskii*, though the single *S. kowalevskii* orthologue of *FoxC1* and *FoxC2*—which are expressed in pharyngeal arch mesenchyme in mouse, chicken and frog [56–59]—is expressed in the developing gill pore endoderm in *S. kowalevskii*. Interestingly, expression studies of *FoxC* paralogues in the shark *Scyliorhinus canicula* report that *FoxC1* is expressed in pharyngeal arch mesenchyme, while *FoxC2* is expressed exclusively in pharyngeal endoderm—a site of expression that has not been described in any other vertebrate to date [48]. While Wotton *et al.* [48] consider this endodermal expression of *FoxC2* to be a derived condition of chondrichthyans, our findings hint at a possible primitive role for *FoxC* expression in deuterostome pharyngeal endoderm.

Seemingly coincident with the absence of a molecularly distinct mesoderm population in the developing *S. kowalevskii* pharynx is the conspicuous absence of a discrete mesodermal core in the pharyngeal arches of juvenile *S. kowalevskii*, or mesodermal derivatives within the pharyngeal arches of adult *S. kowalevskii*. The pharyngeal arches of *S. kowalevskii* are bound by epithelium, but are filled largely with metacoel and an acellular collagenous matrix that is secreted by cells of the pharyngeal endoderm [24–28] (figure 6*a*). This condition is markedly different from that seen in the cephalochordate *Branchiostoma lanceolatum* (in which the pharyngeal epithelium encloses paraxial mesoderm; figure 6*b*) or in vertebrates (in which the pharyngeal epithelium encloses a distinct core of paraxial mesoderm and neural crest-derived mesenchyme; figure 6*c*). Experimental embryological data from chick and axolotl suggest that the ability to form pharyngeal endodermal outpockets is an intrinsic property of foregut endoderm, with little dependence upon interactions with adjacent mesoderm or neural-crest-derived mesenchyme [60–62] (though see [63]). Additionally, the presence of gill slits along the entire length of the body—from the mouth to the anus—in certain stem gnathostomes [64] suggests that endodermal outpocketing from the gut can occur regardless of the identity (i.e. paraxial versus lateral plate) of adjacent mesoderm. Based on these observations—and in light of our expression data revealing conservation of vertebrate pharyngeal arch transcription factor expression exclusively in the pharyngeal endoderm of *S. kowalevskii*—we hypothesize that gill slit formation in deuterostomes was primitively an endodermally driven process, and that pharyngeal endodermal outpockets are the level at which hemichordate and vertebrate gills may be considered homologous. The acquisition of cranial paraxial mesoderm and neural-crest-derived mesenchyme within the pharyngeal arches of chordates and vertebrates, respectively, probably provided the basis of novel epithelial–mesenchymal interactions and, consequently, anatomical novelty.

We thank Mike Coates, Victoria Prince, Kate Rawlinson, Neil Shubin and members of the Lowe laboratory for helpful discussion; Clare Baker for hosting J.A.G. during the completion of this work; John Gerhart for assistance with gene cloning; Marc Kirschner and Bob Freeman for bioinformatic support; and the staff of the Marine Biological Laboratory and the Waquoit Bay Estuarine Reserve for technical support during our field seasons. This project was supported by NSERC Postgraduate and Newton International Postdoctoral Fellowships (to J.A.G.), a European Molecular Biology Organization Postdoctoral Fellowship (to J.H.F.) and National Science Foundation (0818679) and Searle Kinship Foundation grants (to C.J.L.).

REFERENCES

1 Gee, H. 1996 *Before the backbone: views on the origins of vertebrates*. London, UK: Chapman and Hall.
2 Gans, C. & Northcutt, R. G. 1983 Neural crest and the origin of vertebrates: a new head. *Science* **220**, 268–273. (doi:10.1126/science.220.4594.268)
3 Gans, C. 1989 Stages in the origin of vertebrates: analysis by means of scenarios. *Biol. Rev.* **64**, 221–268. (doi:10.1111/j.1469-185X.1989.tb00471.x)
4 Mallatt, J. 1996 Ventilation and the origin of jawed vertebrates: a new mouth. *Zool. J. Linn. Soc.* **117**, 329–404. (doi:10.1111/j.1096-3642.1996.tb01658.x)
5 Mallatt, J. 1997 Crossing a major morphological boundary: the origin of jaws in vertebrates. *Zool. Anal. Complex Syst.* **100**, 128–140.
6 Northcutt, R. G. 2005 The new head hypothesis revisited. *J. Exp. Zool. Part B* **304**, 274–297. (doi:10.1002/jez.b.21063)
7 Purnell, M. A. 2002 Feeding in extinct heterostracan fishes and testing scenarios of early vertebrate evolution. *Proc. R. Soc. Lond. B* **269**, 83–88. (doi:10.1098/rspb.2001.1826)
8 Bateson, W. 1885 The later stages in the development of *B. kowaleskii*, with a suggestion as to the affinities of the Enteropneusta. *Quart. J. Microsc. Sci.* **25**(suppl.), 81–122.
9 Clausen, S. & Smith, A. B. 2005 Palaeoanatomy and biological affinities of a Cambrian deuterostome (Stylophora). *Nature* **43**, 351–354. (doi:10.1038/nature04109)
10 Shu, D., Morris, S. C., Zhang, Z. F., Liu, J. N., Han, J., Chen, L., Zhang, X. L., Yasui, K. & Li, Y. 2003 A new species of Yunnanozoan with implications for deuterostome evolution. *Science* **299**, 1380–1384. (doi:10.1126/science.1079846)
11 Hervé, P., Brinkmann, H., Copley, R. R., Moroz, L. L., Nakano, H., Poustka, A. J., Wallberg, A., Peterson, K. L. & Telford, M. J. 2011 Acoelomorph flatworms are deuterostomes related to *Xenoturbella*. *Nature* **470**, 255–258. (doi:10.1038/nature09676)
12 Swalla, B. J. & Smith, A. B. 2008 Deciphering deuterostome phylogeny: molecular, morphological and palaeontological perspectives. *Phil. Trans. R. Soc. B* **363**, 1557–1568. (doi:10.1098/rstb.2007.2246)
13 Graham, A. 2001 The development and evolution of pharyngeal arches. *J. Anat.* **19**, 133–141. (doi:10.1046/j.1469-7580.2001.19910133.x)
14 Trainor, P. A. & Tam, P. P. L. 1995 Cranial paraxial mesoderm and neural crest cells of the mouse embryo: co-distribution in the craniofacial mesenchyme but distinct segregation in the branchial arches. *Development* **121**, 2569–2582.
15 Hacker, A. & Guthrie, S. 1998 A distinct developmental programme for the cranial paraxial mesoderm in the chick embryo. *Development* **125**, 3461–3472.
16 D'Amico-Martel, A. & Noden, D. M. 1983 Contributions of placodal and neural crest cells to avian cranial peripheral ganglia. *Am. J. Anat.* **166**, 445–468. (doi:10.1002/aja.1001660406)
17 Couly, G. & LeDouarin, N. M. 1990 Head morphogenesis in embryonic avian chimeras: evidence for a segmental pattern in the ectoderm corresponding to the neuromeres. *Development* **108**, 543–558.
18 Noden, D. M. 1983 The role of the neural crest in patterning of avian cranial skeletal, connective, and muscle tissues. *Dev. Biol.* **96**, 144–165. (doi:10.1016/0012-1606(83)90318-4)
19 Couly, G., Coltey, P. M. & LeDouarin, N. M. 1993 The triple origin of skull in higher vertebrates: a study in quail-chick chimeras. *Development* **117**, 409–429.
20 LeDouarin, N. M. & Jotereau, F. V. 1975 Tracing of cells of the avian thymus through embryonic life in interspecific chimeras. *J. Exp. Med.* **142**, 17–40. (doi:10.1084/jem.142.1.17)
21 Cordier, A. C. & Haumont, S. M. 1980 Development of thymus, parathyroid and ultimobranchial bodies in NMRI and nude mice. *Am. J. Anat.* **157**, 227–263. (doi:10.1002/aja.1001570303)
22 Rupert, E. E. 2005 Key characters uniting hemichordates and chordates: homologies or homoplasies? *Can. J. Zool.* **83**, 8–23. (doi:10.1139/z04-158)
23 Gonzalez, P. & Cameron, C. B. 2009 The gill slits and pre-oral ciliary organ of Protoglossus (Hemichordata:

Enteropneusta) are filter-feeding structures. *Biol. J. Linn. Soc.* **98**, 898–906. (doi:10.1111/j.1095-8312.2009.01332.x)
24 Pardos, F. & Benito, J. 1988 Blood vessels and related structures in the gill bars of *Glossobalanus minutus* (Enteropneusta). *Acta. Zool.* (*Stockholm*) **68**, 87–94. (doi:10.1111/j.1463-6395.1988.tb00905.x)
25 Balser, E. J. & Ruppert, E. E. 1990 Structure, ultrastructure, and function of the preoral heart-kidney in *Saccoglossus kowalevskii* (Hemichordata, Enteropneusta) including new data on the stomochord. *Acta. Zool. (Stockholm)* **71**, 235–249. (doi:10.1111/j.1463-6395.1990.tb01082.x)
26 Cole, A. G. & Hall, B. K. 2004 The nature and significance of invertebrate cartilages revisited; distribution and histology of cartilage and cartilage-like tissue within the Metazoa. *Zoology* **107**, 261–273. (doi:10.1016/j.zool.2004.05.001)
27 Rychel, A. L., Smith, S. E., Shimamoto, S. T. & Swalla, B. J. 2006 Evolution and development of the chordates: collagen and pharyngeal cartilage. *Mol. Biol. Evol.* **23**, 541–549. (doi:10.1093/molbev/msj055)
28 Rychel, A. L. & Swalla, B. J. 2007 Development and evolution of chordate cartilage. *J. Exp. Zool. Part B* **308**, 325–335. (doi:10.1002/jez.b.21157)
29 Xu, P. X., Zheng, W., Laclef, C., Maire, P., Maas, R. L., Peters, H. & Xu, X. 2002 *Eya1* is required for the morphogenesis of mammalian thymus, parathyroid and thyroid. *Development* **129**, 3033–3044.
30 Wurdak, H., Ittner, L. M. & Sommer, L. 2006 DiGeorge syndrome and pharyngeal apparatus development. *BioEssays* **28**, 1078–1086. (doi:10.1002/bies.20484)
31 Zou, D., Silvius, D., Davenport, J., Grifone, R., Maire, P. & Xu, X. 2006 Patterning of the third pharyngeal pouch into thymus/parathyroid by *Six* and *Eya1*. *Dev. Biol.* **293**, 499–512. (doi:10.1016/j.ydbio.2005.12.015)
32 Lowe, C. J., Tagawa, K., Humphreys, T., Kirschner, M. & Gerhart, J. 2004 Hemichordate embryos: procurement, culture, and basic methods. *Method Cell. Biol.* **74**, 171–194. (doi:10.1016/S0091-679X(04)74008-X)
33 Gillis, J. A., Dahn, R. D. & Shubin, N. H. 2009 Chondrogenesis and homology of the visceral skeleton in the little skate, *Leucoraja erinacea* (Chondrichthyes: Batoidea). *J. Morphol.* **270**, 628–643. (doi:10.1002/jmor.10710)
34 Kowalevsky, A. 1867 Entwickelungsgeschichte des *Amphioxus lanceolatus*. *Mém. Acad. Imp. Sci. St. Petersb.* (*Sér. VII*) **11**, 1–17.
35 Neubüser, A., Koseki, H. & Balling, R. 1995 Characterizations and developmental expression of *Pax9*, a paired-box containing gene related to *Pax1*. *Dev. Biol.* **170**, 701–716. (doi:10.1006/dbio.1995.1248)
36 Wallin, J., Eibel, H., Neubüser, A., Wilting, J., Koseki, H. & Balling, R. 1996 *Pax1* is expressed during development of the thymus epithelium and is required for normal T-cell maturation. *Development* **122**, 23–30.
37 Lowe, C. J., Wu, M., Salic, A., Evans, L., Lander, E., Stange-Thomann, N., Gruber, C. E., Gerhart, J. & Kirschner, M. 2003 Anteroposterior patterning in hemichordates and the origins of the chordate nervous system. *Cell* **113**, 853–865. (doi:10.1016/S0092-8674(03)00469-0)
38 Ogasawara, M., Wada, H., Paters, H. & Satoh, N. 1999 Developmental expression of *Pax1/9* genes in urochordate and hemichordate gills: insight into function and evolution of the pharyngeal epithelium. *Development* **126**, 2539–2550.
39 Manley, N. R. & Capecchi, M. R. 1995 The role of *Hoxa-3* in mouse thymus and thyroid development. *Development* **121**, 1989–2003.
40 Wendling, O., Dennefeld, C., Chambon, P. & Mark, M. 2000 Retinoid signaling is essential for patterning the endoderm of the third and fourth pharyngeal arches. *Development* **127**, 1553–1562.
41 Rossel, M. & Capecchi, M. R. 1999 Mice mutant for both *Hoxa1* and *Hoxb1* show extensive remodeling of the hindbrain and defects in craniofacial development. *Development* **126**, 5027–5040.
42 Aronowicz, J. & Lowe, C. J. 2006 *Hox* gene expression in the hemichordate *S. kowalevskii* and the evolution of deuterostome nervous systems. *Integr. Comp. Biol.* **46**, 890–901. (doi:10.1093/icb/icl045)
43 Chapman, D. L. *et al.* 1996 Expression of the T-box family genes, *Tbx1-Tbx5*, during early mouse development. *Dev. Dyn.* **206**, 379–390. (doi:10.1002/(SICI)1097-0177(199608)206:4<379::AID-AJA4>3.0.CO;2-F)
44 Jerome, L. A. & Papaioannou, V. E. 2001 DiGeorge syndrome phenotype in mice mutant for the T-box gene, *Tbx1*. *Nat. Genet.* **27**, 286–291. (doi:10.1038/85845)
45 Yamagishi, H., Maeda, J., Hu, T., McAnally, J., Conway, S. J., Kume, T., Meyers, E. N., Yamagishi, C. & Srivastava, D. 2003 *Tbx1* is regulated by tissue-specific forkhead proteins through a common Sonic hedgehog-responsive enhancer. *Genes Dev.* **17**, 269–281. (doi:10.1101/gad.1048903)
46 Kume, T., Jiang, H., Topczewska, J. M. & Hogan, B. L. M. 2001 The murine winged helix transcription factors, *Foxc1* and *Foxc2*, are both required for cardiovascular development and somitogenesis. *Genes Dev.* **15**, 2470–2482. (doi:10.1101/gad.907301)
47 Seo, S. & Kume, T. 2006 Forkhead transcription factors, *Foxc1* and *Foxc2*, are required for the morphogenesis of the cardiac outflow tract. *Dev. Biol.* **296**, 421–436. (doi:10.1016/j.ydbio.2006.06.012)
48 Wotton, K. R., Mazet, F. & Shimeld, S. M. 2008 Expression of FoxC, FoxF, FoxL1, and FoxQ1 genes in the dogfish *Scyliorhinus canicula* defines ancient and derived roles for fox genes in vertebrate development. *Dev. Dyn.* **237**, 1590–1603. (doi:10.1002/dvdy.21553)
49 Holland, L. Z. & Holland, N. D. 1996 Expression of *AmphiHox-1* and *AmphiPax-1* in amphioxus embryos treated with retinoic acid: insights into evolution and patterning of the chordate nerve cord and pharynx. *Development* **122**, 1829–1838.
50 Kozmik, Z. *et al.* 2007 *Pax-Six-Eya-Dach* network during amphioxus development: conservation *in vitro* but context specificity *in vivo*. *Dev. Biol.* **306**, 143–159. (doi:10.1016/j.ydbio.2007.03.009)
51 Chisaka, O. & Capecchi, M. R. 1991 Regionally restricted developmental defects resulting from targeted disruption of the mouse homeobox gene *hox-1.5*. *Nature* **350**, 473–479. (doi:10.1038/350473a0)
52 Kameda, Y., Nishimaki, T., Takeichi, M. & Chisaka, O. 2002 Homeobox gene *Hoxa3* is essential for the formation of the carotid body in the mouse embryos. *Dev. Biol.* **247**, 197–209. (doi:10.1006/dbio.2002.0689)
53 Schubert, M., Yu, J.-K., Holland, N. D., Escriva, H., Laudet, V. & Holland, L. Z. 2005 Retinoic acid signaling acts via *Hox1* to establish the posterior limit of the pharynx in the chordate amphioxus. *Development* **132**, 61–73. (doi:10.1242/dev.01554)
54 Sauka-Spengler, T., Le Mentec, C., Lepage, M. & Mazan, S. 2002 Embryonic expression of *Tbx1*, a DiGeorge syndrome candidate gene, in the lamprey *Lampetra fluviatilis*. *Gene Exp. Patterns* **2**, 99–103. (doi:10.1016/S0925-4773(02)00301-5)
55 Mahadevan, N. R., Horton, A. C. & Gibson-Brown, J. J. 2004 Developmental expression of the amphioxus *Tbx1/10*

gene illuminates the evolution of vertebrate branchial arches and sclerotome. *Dev. Genes Evol.* **214**, 559–566. (doi:10.1007/s00427-004-0433-1)
56 Buchberger, A., Schwarzer, M., Brand, T., Pabst, O., Seidl, K. & Arnold, H. H. 1998 Chicken winged-helix transcription factor cFKH-1 prefigures axial and appendicular skeletal structures during chicken embryogenesis. *Dev. Dyn.* **212**, 94–101. (doi:10.1002/(SICI)1097-0177(199805)212:1<94::AID-AJA9>3.0.CO;2-Y)
57 Iida, K. *et al.* 1997 Essential roles of the winged helix transcription factor MFH-1 in aortic arch patterning and skeletogenesis. *Development* **124**, 4627–4638.
58 Koster, M., Dillinger, K. & Knochel, W. 1998 Expression pattern of the winged helix factor XFD-11 during *Xenopus* embryogenesis. *Mech. Dev.* **76**, 169–173. (doi:10.1016/S0925-4773(98)00123-3)
59 Winnier, G. E., Kume, T., Deng, K., Rogers, R., Bundy, J., Raines, C., Walter, M. A., Hogan, B. L. & Conway, S. J. 1999 Roles for the winged helix transcription factors MF1 and MFH1 in cardiovascular development revealed by nonallelic noncomplementation of null alleles. *Dev. Biol.* **21**, 418–431.
60 Müller, T. S., Ebensperger, C., Neubüser, A., Koseki, H., Balling, R., Christ, B. & Wilting, J. 1996 Expression of avian *Pax1* and *Pax9* is intrinsically regulated in the pharyngeal endoderm, but depends on environmental influences in the paraxial mesoderm. *Dev. Biol.* **178**, 403–417. (doi:10.1006/dbio.1996.0227)
61 Hörstadius, S. & Sellman, S. 1946 Experimentelle Untersuchungen über die Determination des knorpeligen Kopfskelletes bei Urodelen. *Nov. Act. Reg. Soc. Scient. Ups. Ser. IV* **13**, 1–170.
62 Veitch, E., Begbie, J., Schilling, T. F., Smith, M. M. & Graham, A. 1999 Pharyngeal arch patterning in the absence of neural crest. *Curr. Biol.* **9**, 1481–1484. (doi:10.1016/S0960-9822(00)80118-9)
63 Quinlan, R., Gale, E., Maden, M. & Graham, A. 2002 Deficits in the posterior pharyngeal endoderm in the absence of retinoids. *Dev. Dyn.* **225**, 54–60. (doi:10.1002/dvdy.10137)
64 Janvier, P. & Arsenault, M. 2007 The anatomy of *Euphanerops longaevus* Woodward, 1900 an anaspid-like jawless vertebrate from the Upper Devonian of Miguasha, Quebec, Canada. *Geodiversitas* **29**, 143–216.